

Dynamic contact response of a finite beam on a tensionless Pasternak foundation under symmetric and asymmetric loading

İrfan Coşkun[†]

*Faculty of Civil Engineering, Yıldız Technical University, Davutpasa Campus,
34210 Esenler, İstanbul, Turkey*

(Received May 13, 2009, Accepted November 6, 2009)

Abstract. The dynamic response of a finite Bernoulli-Euler beam resting on a tensionless Pasternak foundation and subjected to a concentrated harmonic load is investigated in this study. This load may be applied at the center of the beam, or it may be offset from the center. Since the elastic foundation is assumed to be tensionless, the beam may lift off the foundation, resulting in contact and non-contact regions in the system. An analytical/numerical solution is obtained from the governing equations of the contact and non-contact regions to determine the coordinates of the lift-off points. Although there is no nonlinear term in the equations, the problem appears to be nonlinear since the contact regions are not known in advance. Due to that nonlinearity, the essentials of the problem (the coordinates of the lift-off points) are calculated numerically using the Newton-Raphson technique. The results, which represent the symmetric and asymmetric responses of the beam, are presented graphically in this work. They illustrate the effects of the forcing frequency and the beam length on the extent of the contact regions and displacements.

Keywords: finite beam; Pasternak foundation; lift-off; harmonic load.

1. Introduction

Vibration problems of beams or beam-columns on elastic foundations are important in many fields of structural and foundation engineering. As the mechanical response of the foundation is governed by many factors and cannot be calculated directly, it is necessary to model the foundation behavior. The Winkler elastic foundation model, which consists of an infinite number of closed-spaced linear springs, is a one-parameter model used extensively in practice. The well-known text by Hetenyi (1946) provides a thorough treatment of the Winkler model for elastic foundations. Although the model is simple and widely used, it does not accurately characterize many practical foundations since it does not consider the interactions between the springs. To overcome this dilemma, several two-parameter foundation models have been suggested. A comprehensive review of these models was presented by Kerr (1964), Zhaohua and Cook (1983), and recently by Dutta and Roy (2002). In this paper, Pasternak's model will be employed to represent the foundation, in which the shear

[†] Associate Professor, E-mail: coskun@yildiz.edu.tr

interaction between the springs is considered. This is accomplished by connecting the top ends of the springs to an incompressible layer that resists only transverse shear deformations.

In most studies on the static and dynamic behaviors of beams on an elastic foundation, it is assumed that the foundation (regardless of whether the model is of the Winkler or two-parameter variety) reacts in tension as well as in compression. That is, if a downward lateral load is applied to a beam resting on a foundation, the beam will be compressed into the foundation. If the direction of the load is reversed, the beam and the foundation are pulled up, creating tension in the foundation. However, this assumption does not hold for many practical problems; i.e., while compressive stresses can be transmitted easily, it is difficult to transmit tensile stresses across the boundary between a beam and foundation except when the adhesion between the beam and the foundation is assured, and no separation is thus permitted between them. Instead, a model in which the foundation reacts only by compression (one-way or tensionless) is more realistic. In the case of an absence of tensile forces across the interface between the beam and the foundation, lift-off regions can develop in the system. The problem of beams resting on a tensionless foundation is complicated since the location and the extent of the contact/lift-off regions are not known at the outset. Thus, even for cases involving linear foundation models and linear beam theories, the problem is nonlinear and must be solved iteratively.

The dynamics and stability of beams have been extensively studied by many researchers using the conventional Winkler foundation. However, the case of beams on two-parameter foundations has received less attention due to the model complexity and the difficulties in the parameter value estimation. Typical studies on this subject can be found in studies by Valsangkar and Pradhanang (1988), Franciosi and Masi (1993), De Rosa (1995), De Rosa and Maurizi (1998), Horibe and Asano (2001), Filipich and Rosales (2002), Rao (2003), Chen *et al.* (2004), and Malekzadeh and Karami (2008). Although there are extensive analyses of beams on elastic foundations that react in compression and tension, only a limited number of studies addressing tensionless foundations have been published. The static/dynamic behavior of infinite beams resting on a tensionless foundation has been studied by Tsai and Westmann (1967), Weitsman (1970, 1971, 1972), Rao (1974), Choros and Adams (1979), Lin and Adams (1987), Ioakimidis (1996), and Maheshwari *et al.* (2004). In these studies, due to the infinite beam assumption, the system is symmetric and the applied concentrated load must be centered on the beam.

There are some studies involving the performance of finite beams on tensionless foundations. Celep *et al.* (1989) studied the dynamic response of a finite beam on a tensionless Winkler foundation by considering eccentric loading. Kerr and Coffin (1991) studied the static behavior of a finite beam resting on a tensionless Pasternak foundation subjected to a vertical concentrated load. Kaschiev and Mikhajlov (1995) studied the problem of elastic beams on a tensionless Winkler foundation for arbitrary loads. Coşkun and Engin (1999), and Coşkun (2000) studied the forced vibrations of a finite beam resting on a nonlinear tensionless Winkler foundation subjected to a vertical concentrated load. Coşkun (2003) studied the response of a finite beam on a tensionless Pasternak foundation subjected to a vertical harmonic load. Zhang and Murphy (2004) studied the static response of a finite beam resting on a tensionless Winkler foundation subjected to a vertical concentrated load that could be applied symmetrically or asymmetrically. Celep and Demir (2005) studied the static behavior of a rigid circular beam on a tensionless two-parameter elastic foundation subjected a concentrated force and a moment. The same authors also studied the response of an elastic beam on this type of foundation subjected to a uniformly distributed load and concentrated edge loads (Celep and Demir 2007). Lancioni and Lenci (2007) studied the forced vibrations of a

semi-infinite beam on a tensionless Winkler foundation subjected to a uniformly distributed load. Silveira *et al.* (2008) investigated the static behavior of beams, columns, and arches on this type of foundation under different loading cases. Zhang (2008) studied the static response of a pinned-pinned beam resting on a tensionless Reissner foundation subjected to a concentrated load, which could be applied symmetrically or asymmetrically. By considering the same loading case but a tensionless Pasternak foundation, the free-free beam response was studied by Coşkun *et al.* (2008). Most of the above results include the determination of the coordinates of the lift-off points; i.e., the contact lengths of the beam.

This paper investigates the response of a finite, free-free beam on a tensionless Pasternak foundation subjected to a harmonic concentrated load. This load may either be located at the center of the beam or it may be offset. The off-center loading disrupts the symmetry of the system and requires the specification of appropriate boundary conditions. Closed-form solutions of the differential equations of motion, in each of the contact and non-contact regions are determined, using the coordinate system centered at the load. The boundary and continuity conditions are then satisfied, which leads to a system of algebraic equations that are linear in certain unknown coefficients and nonlinear in the unknown contact region lengths. Elimination of the linear coefficients allows the contact region lengths to be determined numerically from the resulting transcendental equations.

2. Problem formulation

2.1 Definition of the system and governing equations

Consider a finite Bernoulli-Euler beam of length L resting on a tensionless Pasternak foundation and subjected to a vertical load $P(t) = P_0 \cos \Omega t$ such that lift-off of the beam is possible (Fig. 1). The distance to the left (right) end of the beam is L_1 (L_2) and is measured from the origin of the coordinate system centered at the load. The vertical displacement is given by $W(x, t)$. The contact region is defined as $-X_1 < x < X_2$, where X_1 and X_2 represent the lift-off points on the left and right sides of the beam, respectively. In order to investigate the behavior in both the contact and non-

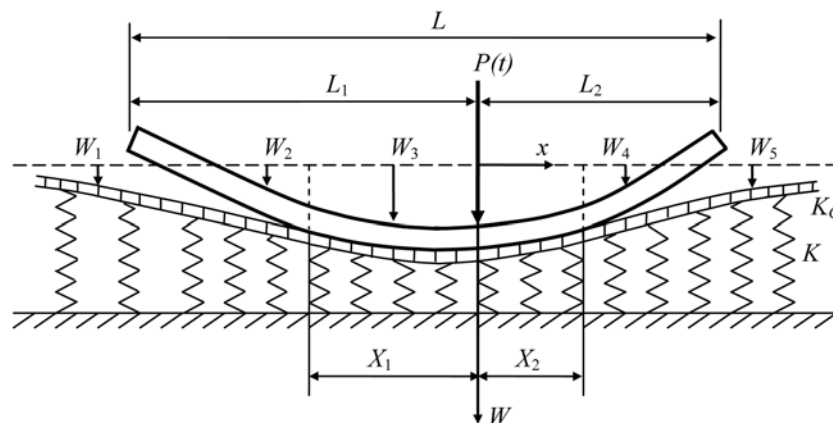


Fig. 1 Beam on a tensionless Pasternak foundation subjected to an eccentric load

contact regions, the vertical displacement $W(x, t)$ is broken into the following five distinct regions

$$W(x, t) = \begin{cases} W_1, & -\infty < x < -X_1 \\ W_2, & -L_1 < x < -X_1 \\ W_3, & -X_1 < x < -X_2 \\ W_4, & X_2 < x < L_2 \\ W_5, & X_2 < x < \infty \end{cases}$$

where $W_1(W_5)$ and $W_2(W_4)$ are the displacements in the non-contact regions for the foundation surface and the beam, respectively, and W_3 is the displacement in the contact region. The governing equations for these regions are

$$G \frac{\partial^2 W_1}{\partial x^2} - kW_1 = m_f \frac{\partial^2 W_1}{\partial t^2}, \quad -\infty < x < -X_1 \quad (1)$$

$$EI \frac{\partial^4 W_2}{\partial x^4} = -m_b \frac{\partial^2 W_2}{\partial t^2}, \quad -L_1 < x < -X_1 \quad (2)$$

$$EI \frac{\partial^4 W_3}{\partial x^4} - G \frac{\partial^2 W_3}{\partial x^2} + kW_3 = -(m_f + m_b) \frac{\partial^2 W_3}{\partial t^2} + P_0 \delta(x) \cos \Omega t, \quad -X_1 < x < -X_2 \quad (3)$$

$$EI \frac{\partial^4 W_4}{\partial x^4} = -m_b \frac{\partial^2 W_4}{\partial t^2}, \quad X_2 < x < L_2 \quad (4)$$

$$G \frac{\partial^2 W_5}{\partial x^2} - kW_5 = m_f \frac{\partial^2 W_5}{\partial t^2}, \quad X_2 < x < \infty \quad (5)$$

where k is the Winkler foundation modulus, G is the shear modulus of the shear layer, Ω is the forcing frequency, P_0 is the forcing amplitude, EI is the beam flexural rigidity, $\delta(x)$ is the Dirac delta function, and m_b and m_f are the masses per unit length of the beam and foundation, respectively. In the formulation given above, it is assumed that: (i) both the beam and foundation are isotropic, homogeneous and linearly elastic; (ii) the vibration amplitudes of the system are sufficiently small; and (iii) the effect of damping is neglected. Since the forcing is harmonic in time, and thus the response of the beam and the foundation is harmonic, the displacements can be written as

$$W_i(x, t) = W_i(x) \cos \Omega t, \quad i = 1-5 \quad (6)$$

For convenience, the non-dimensionalized variable ξ , displacement $w(\xi)$, Winkler foundation constant λ , shear foundation coefficient λ_G , frequency parameter $\bar{\Omega}$, mass ratio \bar{m} , load F , lift-off points ξ_1 and ξ_2 , beam length l , and left (right) side beam length $l_1(l_2)$ are introduced as follows

$$\begin{aligned} \lambda^4 &= \frac{k}{4EI}, \quad \xi = \lambda x, \quad \xi_1 = \lambda X_1, \quad \xi_2 = \lambda X_2, \quad l = \lambda L, \quad l_1 = \lambda L_1, \quad l_2 = \lambda L_2 \\ w &= \lambda W, \quad \lambda_G = \frac{k}{G\lambda^2}, \quad F = \frac{P_0}{\lambda^2 4EI}, \quad \bar{\Omega}^2 = \frac{m_b}{k} \Omega^2, \quad \bar{m} = \frac{m_b}{m_f} \end{aligned} \quad (7)$$

Introducing these quantities into the governing Eqs. (1)-(5) produces the following non-dimensional equations

$$\frac{d^2 w_1}{d\xi^2} - \lambda_G \left(1 - \frac{\bar{\Omega}^2}{m}\right) w_1 = 0, \quad -\infty < \xi < -\xi_1 \tag{8}$$

$$\frac{d^4 w_2}{d\xi^4} - (4\bar{\Omega}^2) w_2 = 0, \quad -l_1 < \xi < -\xi_1 \tag{9}$$

$$\frac{d^4 w_3}{d\xi^4} - \frac{4}{\lambda_G} \frac{d^2 w_3}{d\xi^2} + 4 \left[1 - \left(1 + \frac{1}{m}\right) \bar{\Omega}^2\right] w_3 = F\delta(\xi), \quad -\xi_1 < \xi < \xi_2 \tag{10}$$

$$\frac{d^4 w_4}{d\xi^4} - (4\bar{\Omega}^2) w_4 = 0, \quad \xi_2 < \xi < l_2 \tag{11}$$

$$\frac{d^2 w_5}{d\xi^2} - \lambda_G \left(1 - \frac{\bar{\Omega}^2}{m}\right) w_5 = 0, \quad \xi_2 < \xi < \infty \tag{12}$$

2.2 Boundary conditions

Eqs. (8) and (12) are second order differential equations and Eqs. (9), (10), and (11) are fourth order differential equations. Therefore, 16 integration constants will appear in the solution of these equations. Because the lift-off points (ξ_1, ξ_2) are also unknown, there are a total of 18 unknowns to be determined. To obtain them, there must be an equal number of boundary/matching conditions. At $\xi = -\xi_1$ and $\xi = \xi_2$, the geometric boundary conditions require continuity of the displacement and slope. These are expressed as

$$w_1(-\xi_1) = w_3(-\xi_1), \quad \frac{dw_1(-\xi_1)}{d\xi} = \frac{dw_3(-\xi_1)}{d\xi}, \quad w_2(-\xi_1) = w_3(-\xi_1), \quad \frac{dw_2(-\xi_1)}{d\xi} = \frac{dw_3(-\xi_1)}{d\xi} \tag{13}$$

$$w_3(\xi_2) = w_5(\xi_2), \quad \frac{dw_3(\xi_2)}{d\xi} = \frac{dw_5(\xi_2)}{d\xi}, \quad w_3(\xi_2) = w_4(\xi_2), \quad \frac{dw_3(\xi_2)}{d\xi} = \frac{dw_4(\xi_2)}{d\xi} \tag{14}$$

There are also four natural boundary conditions at $\xi = -\xi_1, \xi_2$. These conditions require continuity of the bending moment and shear force. These are

$$\frac{d^2 w_2(-\xi_1)}{d\xi^2} = \frac{d^2 w_3(-\xi_1)}{d\xi^2}, \quad \frac{d^3 w_2(-\xi_1)}{d\xi^3} = \frac{d^3 w_3(-\xi_1)}{d\xi^3} \tag{15}$$

$$\frac{d^2 w_3(\xi_2)}{d\xi^2} = \frac{d^2 w_4(\xi_2)}{d\xi^2}, \quad \frac{d^3 w_3(\xi_2)}{d\xi^3} = \frac{d^3 w_4(\xi_2)}{d\xi^3} \tag{16}$$

At $\xi = -l_1$ and $\xi = l_2$, there is no bending moment or shear force. Thus, the natural boundary conditions at these points can be written as

$$\frac{d^2 w_2(-l_1)}{d\xi^2} = 0, \quad \frac{d^3 w_2(-l_1)}{d\xi^3} = 0, \quad \frac{d^2 w_4(l_2)}{d\xi^2} = 0, \quad \frac{d^3 w_4(l_2)}{d\xi^3} = 0 \tag{17}$$

Finally, the displacement $w(\xi)$ at the free foundation surface should be finite as $\xi \rightarrow \pm\infty$. This gives us two additional conditions

$$\lim_{\xi \rightarrow -\infty} \{w_1\} \rightarrow \text{finite}, \quad \lim_{\xi \rightarrow \infty} \{w_5\} \rightarrow \text{finite} \quad (18)$$

These are the 18 boundary/matching conditions necessary to determine the 18 unknown constants. However, in the formulation given above, it is assumed that the load may either be applied at the center of the beam or be offset. If the load is applied at the center of the beam, the number of the boundary/matching conditions reduces to 11 with the use of the symmetry in the system. If the $\xi \geq 0$ region is considered, for instance, the boundary and matching conditions given above for the right side of the system are still valid. However, in addition to these conditions, one must use the continuity of the slope of the elastic curve and the symmetry in the system: i.e., in dimensional terms, the slope is zero ($W_3'(0) = 0$) and the shear force is $W_3'''(0) = P/(2EI)$ at the center of the beam. Apart from this, in some cases, the beam may be completely compressed into the foundation (no separation develops), or one-sided contact may occur between the beam and the foundation. In the full contact case, the slopes of the free part of the foundation and the foundation beneath the beam are not equal at the free ends of the beam. Thus, the boundary conditions that will be satisfied at $\xi = -l_1$ and $\xi = l_2$ are

$$-\frac{d^3 w_3(-l_1)}{d\xi^3} + \frac{4}{\lambda_G} \frac{dw_3(-l_1)}{d\xi} = \frac{4}{\lambda_G} \frac{dw_1(-l_1)}{d\xi}, \quad -\frac{d^3 w_3(l_2)}{d\xi^3} + \frac{4}{\lambda_G} \frac{dw_3(l_2)}{d\xi} = \frac{4}{\lambda_G} \frac{dw_5(l_2)}{d\xi} \quad (19)$$

Here, the terms on the left and right sides show the generalized shearing force in the foundation beneath the beam and the generalized shearing force in the free part of the foundation, respectively. If one-sided contact occurs in the system, the first or the second sections of Eq. (19) can be used, depending on the region where separation fails to develop. It should be noted here that due to the harmonic excitation, the beam can separate from the foundation completely. In such a case, the governing equation of the beam becomes $w''''(\xi) - 4\bar{\Omega}^2 w(\xi) = F\delta(\xi)$, and can be solved, for example, using the Green's function approach with the appropriate boundary/continuity conditions and the jump condition on the shear.

3. Solution

The differential Eqs. (8)-(12) contain only constant coefficients and are homogeneous except for Eq. (10). By considering the homogeneous form of Eq. (10), solutions to these equations can be taken as

$$w_1(w_5) = A e^{r\xi}, \quad w_2(w_4) = B e^{\theta\xi}, \quad w_3 = C e^{m\xi} \quad (20)$$

Substituting these solutions into Eqs. (8)-(12), one obtains the following characteristic equations

$$r^2 - \lambda_G \left(1 - \frac{\bar{\Omega}^2}{m}\right) = 0 \quad (21)$$

$$\theta^4 - (4\bar{\Omega}^2) = 0 \quad (22)$$

$$m^4 - \left(\frac{4}{\lambda_G}\right)m^2 + 4\left[1 - \left(1 + \frac{1}{\bar{m}}\right)\bar{\Omega}^2\right] = 0 \tag{23}$$

The roots of these equations are

$$r_{1,2} = \pm \sqrt{\lambda_G \left(1 - \frac{\bar{\Omega}^2}{\bar{m}}\right)} \tag{24}$$

$$\theta_{1,2} = \pm \sqrt{2\bar{\Omega}^2}, \quad \theta_{3,4} = \pm i\sqrt{2\bar{\Omega}^2} \tag{25}$$

$$m_{1,2,3,4} = \pm \sqrt{\left(\frac{2}{\lambda_G}\right) \pm \sqrt{\alpha}} \tag{26}$$

where $i = \sqrt{-1}$ and $\alpha = (2/\lambda_G)^2 - 4[1 - (1 + 1/\bar{m})\bar{\Omega}^2]$. Since the parameters EI , k , and G are rigidity parameters of the beam and foundation, they are all non-negative and thus the parameter λ_G is always positive. For this reason, the solutions of Eqs. (8), (10), and (12) depend on whether the values of the roots r and m are real, imaginary, or complex. Taking $\bar{m} = 1$ ($m_b = m_f$) in order to reduce the number of the parameters in the problem, the corresponding solutions to these cases can be written as follows:

Case 1

The roots r_i and m_i are real and unequal if $\bar{\Omega} < (1/\sqrt{2})$ and $\alpha > 0$. In this case, the general solutions of Eqs. (8)-(12) are

$$w_1(\xi) = A_1 e^{\mu\xi} + A_2 e^{-\mu\xi} \tag{27}$$

$$w_2(\xi) = B_1 \cosh \theta\xi + B_2 \sinh \theta\xi + B_3 \cos \theta\xi + B_4 \sin \theta\xi \tag{28}$$

$$w_3(\xi) = C_1 \cosh m_{11}\xi + C_2 \sinh m_{11}\xi + C_3 \cosh m_{12}\xi + C_4 \sinh m_{12}\xi + P_1 \sinh |m_{11}\xi| - P_2 \sinh |m_{12}\xi| \tag{29}$$

$$w_4(\xi) = D_1 \cosh \theta\xi + D_2 \sinh \theta\xi + D_3 \cos \theta\xi + D_4 \sin \theta\xi \tag{30}$$

$$w_5(\xi) = E_1 e^{\mu\xi} + E_2 e^{-\mu\xi} \tag{31}$$

Case 2

The roots r_i are real, and m_i are real and equal if $\bar{\Omega} < (1/\sqrt{2})$ and $\alpha = 0$. The general solution of Eq. (10) is

$$w_3(\xi) = (C_1 + C_2\xi)e^{m_{21}\xi} + (C_3 + C_4\xi)e^{-m_{21}\xi} - P_3 e^{|m_{21}\xi|} + P_4 |\xi| e^{-|m_{21}\xi|} \tag{32}$$

The solutions of Eqs. (8), (9), (11) and (12) are the same as in the *case 1*.

Case 3

The roots r_i and m_i are real and complex, respectively, if $\bar{\Omega} < (1/\sqrt{2})$ and $\alpha < 0$. The general solution of Eq. (10) is

$$w_3(\xi) = (C_1 \cos m_{31}\xi + C_2 \sin m_{31}\xi) \cosh m_{32}\xi + (C_3 \cos m_{31}\xi + C_4 \sin m_{31}\xi) \sinh m_{32}\xi \\ + P_5 \sinh |m_{32}\xi| \cos m_{31}\xi + P_6 \cosh m_{32}\xi \sin |m_{31}\xi| \quad (33)$$

The solutions to Eqs. (8), (9), (11), and (12) are the same as in *case 1*.

Case 4

The roots r_i and two of the roots m_i are real, the other two roots of m_i are imaginary if $(1/\sqrt{2}) < \bar{\Omega} < 1$ and $\alpha > 0$. The general solution of Eq. (10) is

$$w_3(\xi) = C_1 \cosh m_{41}\xi + C_2 \sinh m_{41}\xi + C_3 \cos m_{42}\xi + C_4 \sin m_{42}\xi \\ + P_7 \sinh |m_{41}\xi| - P_8 \sin |m_{42}\xi| \quad (34)$$

Again, the solutions to Eqs. (8), (9), (11), and (12) are the same as in *case 1*.

Case 5

The roots r_i and two of m_i are imaginary, and the two of m_i are real if $\bar{\Omega} > 1$ and $\alpha > 0$. In this case, the general solutions of Eqs. (8) and (12) are

$$w_1(\xi) = A_1 e^{-i\chi\xi} + A_2 e^{i\chi\xi} \quad (35)$$

$$w_5(\xi) = E_1 e^{-i\chi\xi} + E_2 e^{i\chi\xi} \quad (36)$$

While the solutions of (9) and (11) are the same as for *case 1*, the solution to Eq. (10) is equal to that in *case 4*.

In the above solutions, $A_j(E_j)$ ($j = 1, 2$) and B_i, C_i, D_i ($i = 1-4$) are the integration constants. Additionally, the non-dimensional parameters used in these equations are defined as

$$\mu = \sqrt{\lambda_G(1 - \bar{\Omega}^2)}, \quad m_{11} = \sqrt{(2/\lambda_G) + \sqrt{\alpha}}, \quad m_{12} = \sqrt{(2/\lambda_G) - \sqrt{\alpha}}, \quad m_{21} = \sqrt{2/\lambda_G} \\ m_{31} = \sqrt{-(1/\lambda_G) + \sqrt{1 - 2\bar{\Omega}^2}}, \quad m_{32} = \sqrt{(1/\lambda_G) + \sqrt{1 - 2\bar{\Omega}^2}}, \quad m_{41} = \sqrt{(2/\lambda_G) + \sqrt{\alpha}} \\ m_{42} = \sqrt{-(2/\lambda_G) + \sqrt{\alpha}}, \quad \chi = \sqrt{\lambda_G(\bar{\Omega}^2 - 1)}, \quad P_1 = F/2m_{11}(m_{11}^2 - m_{12}^2) \\ P_2 = (m_{11}/m_{12})P_1, \quad P_3 = F/4m_{21}^3, \quad P_4 = m_{21}P_3, \quad P_5 = -F/4m_{32}(m_{32}^2 + m_{31}^2) \\ P_6 = -(m_{32}/m_{31})P_5, \quad P_7 = F/2m_{41}(m_{41}^2 + m_{42}^2), \quad P_8 = (m_{41}/m_{42})P_7 \quad (37)$$

in which the parameters P_1-P_8 are related to the particular solutions of $w_3(\xi)$. The parameters P_5 and P_6 , which are seen in Eq. (33), for example, are obtained as follows. The homogeneous solution of Eq. (10) is

$$(w_3)_h = (C_1 \cos m_{31}\xi + C_2 \sin m_{31}\xi) \cosh m_{32}\xi + (C_3 \cos m_{31}\xi + C_4 \sin m_{31}\xi) \sinh m_{32}\xi \quad (38)$$

Now, consider the particular solution of Eq. (10) to be the sum of the functions $f_1 = P_5 \sinh |m_{32}\xi| \cos(m_{31}\xi)$ and $f_2 = P_6 \cosh(m_{32}\xi) \sin |m_{31}\xi|$. The second and fourth derivatives of these functions with $d|\xi|/d\xi = \text{sgn}(\xi)$ and $d\text{sgn}(\xi)/d\xi = 2\delta(\xi)$ are

$$\begin{aligned}
 f_1'' &= P_5 \left\{ 2 m_{32} \delta(\xi) + \left[-2 m_{32} m_{31} \cosh(m_{32} \xi) \sin |m_{31} \xi| + (m_{32}^2 - m_{31}^2) \sinh |m_{32} \xi| \cos(m_{31} \xi) \right] \right\} \\
 f_1'''' &= P_5 \left\{ 2 m_{32} \delta''(\xi) + 2(m_{32}^3 - 3 m_{32} m_{31}^2) \delta(\xi) + [(4 m_{32}^3 m_{31}^3 - 4 m_{32}^3 m_{31}) \cosh m_{32} \xi \sin |m_{31} \xi| \right. \\
 &\quad \left. + (m_{32}^4 + m_{31}^4 - 6 m_{32}^2 m_{31}^2) \sinh |m_{32} \xi| \cos m_{31} \xi] \right\} \\
 f_2'' &= P_6 \left\{ 2 m_{31} \delta(\xi) + \left[2 m_{32} m_{31} \sinh |m_{32} \xi| \cos m_{31} \xi + (m_{32}^2 - m_{31}^2) \cosh m_{32} \xi \sin |m_{31} \xi| \right] \right\} \\
 f_2'''' &= P_6 \left\{ 2 m_{31} \delta''(\xi) + 2(3 m_{32}^2 m_{31} - m_{31}^3) \delta(\xi) + [(4 m_{32}^3 m_{31} - 4 m_{32} m_{31}^3) \sinh |m_{32} \xi| \cos m_{31} \xi \right. \\
 &\quad \left. + (m_{32}^4 + m_{31}^4 - 6 m_{32}^2 m_{31}^2) \sinh m_{32} \xi \sin |m_{31} \xi|] \right\}
 \end{aligned}$$

Substituting the functions f_1 and f_2 , and the derivatives given above into Eq. (10), and equating the coefficients of $\delta(\xi)$ and $\delta''(\xi)$, one obtains $P_5 = -F/4m_{32}(m_{32}^2 + m_{31}^2)$ and $P_6 = -(m_{32} + m_{31})P_5$. This procedure has been applied for the evaluation of other P_i values.

There are 16 unknown integration constants for any one of the five cases given above. In addition to these constants, the size of the contact zone, given by ξ_1 and ξ_2 , is also unknown. Therefore, the total number of unknowns becomes 18 as was mentioned in section 2. Because the solution procedure for obtaining these unknowns is the same for cases 1-4, only case 1 will be discussed for brevity. However, it should be noted here that the solutions (35) and (36) have exponential spatial behavior on the free foundation surface and correspond to the incoming and outgoing waves when the time factor $e^{i\Omega t}$ is considered. Thus, the radiation condition should be used for case 5. The boundary conditions (18) give $A_2 = 0$ and $E_1 = 0$. Thus, the number of the integration constants is reduced to 14. With the use of the boundary conditions (17), the constants $B_3, B_4, D_3,$ and D_4 are obtained in terms of the other constants as $B_3 = f_1(B_1, B_2), B_4 = f_2(B_1, B_2), D_3 = f_3(D_1, D_2),$ and $D_4 = f_4(D_1, D_2)$. In this case there are 12 boundary conditions that have not yet been used. Substituting these constants into the boundary conditions (13), (14), (15), and (16), 12 nonhomogeneous algebraic equations are obtained for the 10 unknown constants $B_1, B_2, C_1, C_2, C_3, C_4, D_1, D_2, A_1$ and E_2 . In these equations, the coefficients of the constants and the terms that appear on the right hand side of the equations are related to ξ_1 , and ξ_2 . Since ξ_1 and ξ_2 are not known in advance, the solution is determined iteratively. First, ξ_1 and ξ_2 are chosen to numerically obtain the 10 constants from the solutions of the 10 equations at each step, and are substituted into the remaining 2 equations. Then, the lift-off points are determined as the roots of these transcendental equations using the Newton-Raphson technique. During the solution, the global equilibrium of the beam is checked by considering the vertical equilibrium of the forces as

$$\frac{F}{4} = \int_{-\xi_1}^{\xi_2} \left[(1 - 2\bar{\Omega}^2) w_3(\xi) - \frac{1}{\lambda_G} \frac{d^2 w_3(\xi)}{d\xi^2} \right] d\xi - \bar{\Omega}^2 \left[\int_{-\xi_1}^{-l_1} w_1(\xi) d\xi + \int_{\xi_2}^{l_2} w_4(\xi) d\xi \right] \tag{39}$$

4. Numerical results and discussion

Numerical results obtained with the above formulation are displayed graphically to show the effects of the frequency parameter and the beam length on the extent of the contact lengths and displacements for the symmetric and asymmetric loading cases. In all figures, the shear foundation

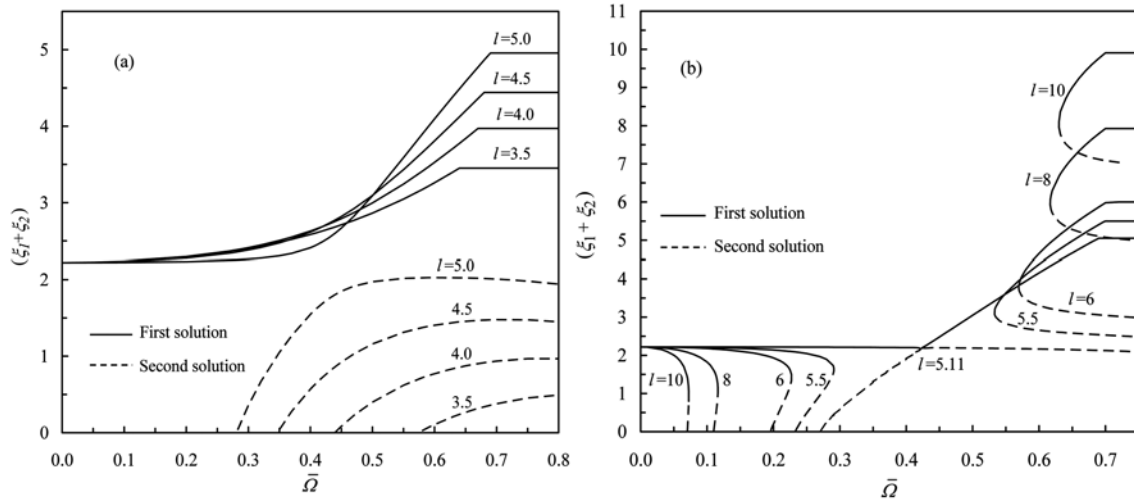


Fig. 2 Variation of total contact length $(\xi_1 + \xi_2)$ as a function of the frequency parameter $\bar{\Omega}$ for different beam lengths l , for the symmetric case ($l_1 = 0.5l$)

coefficient is assumed to be constant at $\lambda_G = 2$, and the applied load is taken to be $F = 1$ (except in Fig. 10).

Fig. 2 shows the variation of the total contact length $(\xi_1 + \xi_2)$ with respect to the frequency parameter $\bar{\Omega}$ for different beam lengths. The concentrated load F is symmetric, i.e., at the center of the beam ($l_1 = 0.5l$), so the left- and right-side contact lengths are equivalent ($\xi_1 = \xi_2$). From Fig. 2(a), it is seen that as $\bar{\Omega}$ increases, first one and then two solutions (two different contact lengths at a fixed $\bar{\Omega}$) develop in the system. In other words, the solution is not unique; for a given beam length and frequency more than one solution exists. The stability of the solutions are not investigated here, but the actual solution can be obtained by using an energy criterion. The contact length increases with the frequency parameter for both solutions. This increase persists until certain values of $\bar{\Omega}$ are reached for the first solution (upper curves in the figure), at which points complete contact develops in the system. These values are $\bar{\Omega} = 0.649$ for $l = 3.5$, 0.674 for $l = 4.0$, 0.687 for $l = 4.5$, and 0.694 for $l = 5.0$. However, for the second solution (lower curves in the figure), the beam continues to separate from the foundation until about $\bar{\Omega} = 0.8$. When $\bar{\Omega}$ is increased beyond this value, first the beam deflections significantly increase (i.e., resonance behavior is seen in the system), and then the contact and non-contact regions are interchanged. In other words, the middle part of the beam lifts off the foundation while the two sides make contact with the foundation. In this case, it is necessary to reformulate the problem with different boundary and continuity conditions, which are given in the Appendix A. In addition to the frequency parameter, the length of the beam considerably affects the contact behavior. As seen in Fig. 2(a), there are one or two solutions in the system for short beam lengths in the $0 \leq \bar{\Omega} \leq 0.8$ region. This situation persists until $l = 5.11$, which is the critical length that changes the qualitative nature of the solution. In other words, there is no solution for some values of the frequency parameter as the beam length increases beyond $l = 5.11$ (Fig. 2(b)). The reason for not having solutions for the low frequency and large beam-length is that at lower frequencies the load exhibits pseudo-static behavior. On the other hand, at large frequencies, the long beam does not have time to react to the load, since the sign of the load quickly changes. Therefore the beam is not lifted much from the foundation, resulting in a

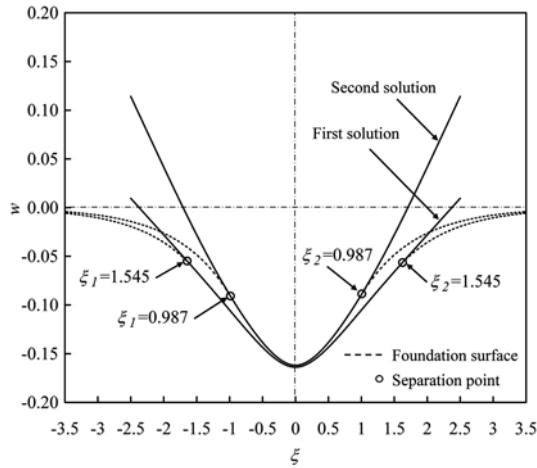


Fig. 3 Deflection curves showing two different lift-off points at the same frequency parameter ($\bar{\Omega} = 0.5$) with $l = 5$ for the symmetric case ($l_1 = 0.5l$)

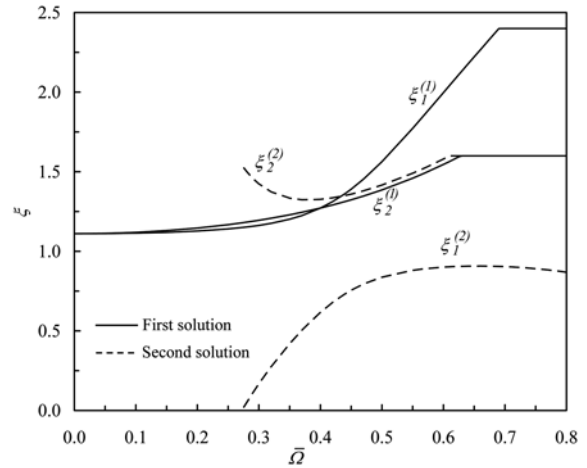


Fig. 4 Variation of the left (ξ_1) and right (ξ_2) side contact lengths as a function of the frequency parameter $\bar{\Omega}$ for $l = 4$, for the asymmetric case ($l_1 = 0.6l$). Note: superscripts (1) and (2) correspond to the first and second solutions, respectively

large contact length. As Fig. 2(b) shows, complete contact develops in the system at higher values of the frequency parameter for the first solution, whereas the contact and non-contact regions interchange for the second solution. As mentioned above, the beam separates from the foundation having two different contact lengths at a fixed frequency (see Fig. 2(a)). An example highlighting this case is given in Fig. 3 with $\bar{\Omega} = 0.5$, for a beam length of $l = 5$. The contact length is $\xi_1 = \xi_2 = 1.545$ for the first solution and $\xi_1 = \xi_2 = 0.987$ for the second solution. The summation of the left and right side contact lengths gives the total contact lengths of the beam as 3.09 and 1.974, respectively, which agrees with Fig. 2(a). It is seen that the first solution gives a larger contact length than that of the second solution.

Fig. 4 shows the variation of the left and right contact lengths with respect to the frequency parameter $\bar{\Omega}$ under an asymmetric loading at $l_1 = 0.6l$, for a relatively small beam length of $l = 4$. For this same length, the symmetric case is given in Fig. 5 for comparison. As seen in Fig. 4, the left ($\xi_1^{(1)}$) and right ($\xi_2^{(1)}$) side contact lengths of the first solution increase as $\bar{\Omega}$ increases, and they reach the left and right side beam lengths ($l_1 = 2.4$; $l_2 = 1.6$) at $\bar{\Omega} = 0.690$ and $\bar{\Omega} = 0.625$, respectively. Due to the asymmetric loading, the right end of the beam touches the foundation before the left end, and after this one-sided lift-off, complete contact develops in the system when the left end touches the foundation. From the figure, it is seen that a second solution develops in the system when $\bar{\Omega} = 0.275$. The corresponding left and right side contact lengths to this solution are $\xi_1^{(2)}$ and $\xi_2^{(2)}$. At $\bar{\Omega} = 0.275$, the left side of the beam is not in contact with the foundation whereas the right side is in full contact ($\xi_2^{(2)} = l_2 = 1.6$). When $\bar{\Omega}$ is increased beyond that value, right side contact length first decreases and then increases until it reaches the right side beam length ($l_2 = 1.6$) at $\bar{\Omega} = 0.610$. The beam continues to separate from the foundation on the left side until about $\bar{\Omega} = 0.8$, i.e., $\xi_1^{(2)}$ does not reach the left side beam length ($l_1 = 2.4$). If the value of $\bar{\Omega}$ is increased beyond that value, the beam deflections increase considerably, and then the contact and non-contact regions interchange, having a one-sided lift-off. In this case, as mentioned previously, it

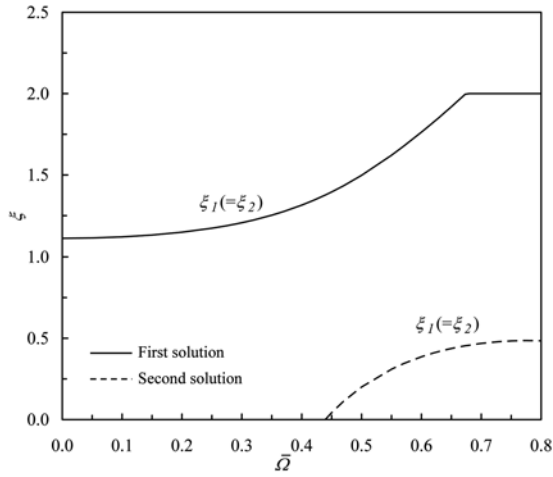


Fig. 5 Variation of the left (ξ_1) side contact lengths as a function of the frequency parameter $\bar{\Omega}$ for $l = 4$, for the symmetric case

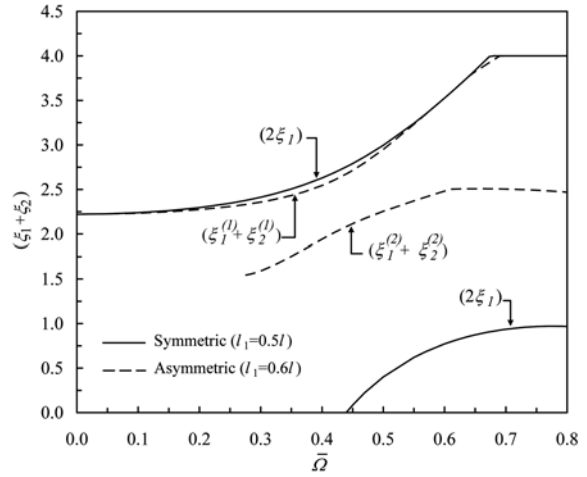


Fig. 6 Variation of total contact length ($\xi_1 + \xi_2$) as a function of the frequency parameter $\bar{\Omega}$ for $l = 4$, for the symmetric and asymmetric case

is necessary to reformulate the problem with different boundary and continuity conditions. These conditions are given in Appendix B for the asymmetric case. By using the contact curves given in Figs. 4 and 5, a comparison of the total contact length of the beam for the symmetric and asymmetric cases is given in Fig. 6. Considering Fig. 5, the total contact length of the beam in the symmetric case ($\xi_1 = \xi_2$) is obtained as $2 \times \xi_1$ for the first and second solutions. However, in the asymmetric case, the total contact length is obtained by summing the left and right contact lengths, since they are different from each other ($\xi_1 \neq \xi_2$). Therefore, the summation of ($\xi_1^{(1)}$) and ($\xi_2^{(1)}$) given in Fig. 4 gives the total contact length for the first solution. Similarly, the summation of ($\xi_1^{(2)}$) and ($\xi_2^{(2)}$) gives the total contact length for the second solution. The contact length in the asymmetric case is smaller than that of the symmetric case for the first solution. This is because the right side contact length in the asymmetric case is always smaller than that of the symmetric one. For example, the left side contact length for the symmetric case is 1.492 at $\bar{\Omega} = 0.5$. Thus, the total contact length is $2 \times \xi_1 = 2.984$. At the same value of $\bar{\Omega}$, the left and right side contact lengths for the asymmetric case are $\xi_1^{(1)} = 1.561$ and $\xi_2^{(1)} = 1.382$, respectively. The total contact length for this case is 2.943. As a result, the contact length is smaller in the asymmetric case than in the symmetric case. In contrast to the first solution, the second solution in the asymmetric case gives larger contact lengths than those in the symmetric case ($\xi_1^{(2)} + \xi_2^{(2)} > 2 \times \xi_1$), since the left and right contact lengths in the asymmetric case are larger.

Fig. 7 shows the deflection curves of the beam ($l = 4$) and the free foundation surface with different frequency parameters for the asymmetric loading case ($l_1 = 0.6l$). For brevity, only the first solution is considered here. The figure shows that the total contact lengths of the beam increase with $\bar{\Omega}$. These are $1.271 + 1.272 = 2.543$ for $\bar{\Omega} = 0.4$, $1.561 + 1.382 = 2.943$ for $\bar{\Omega} = 0.5$, and $2.221 + 1.60 = 3.821$ for $\bar{\Omega} = 0.65$. It is clear that the beam is compressed into the foundation with larger displacements as $\bar{\Omega}$ increases.

As mentioned above, the contact-length behavior changes drastically after the critical beam length ($l = 5.11$), and there is no solution for some ranges of the frequency parameter for long beams in the symmetric case (see Fig. 2(b)). For example, at a beam length of $l = 6$, there is no solution for

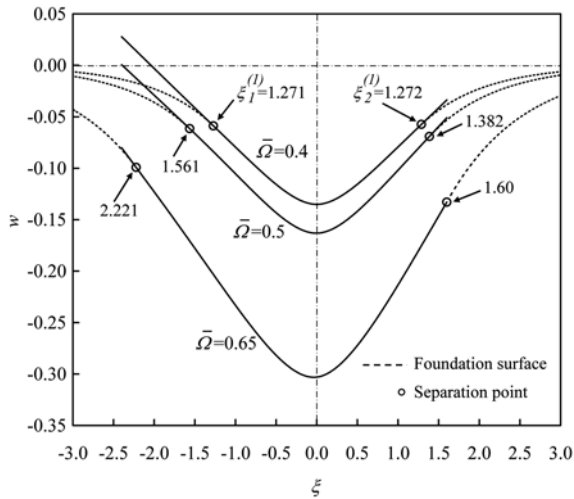


Fig. 7 Deflection curves showing lift-off at different values of the frequency parameter $\bar{\Omega}$ for a beam length of $l = 4$, for the asymmetric case

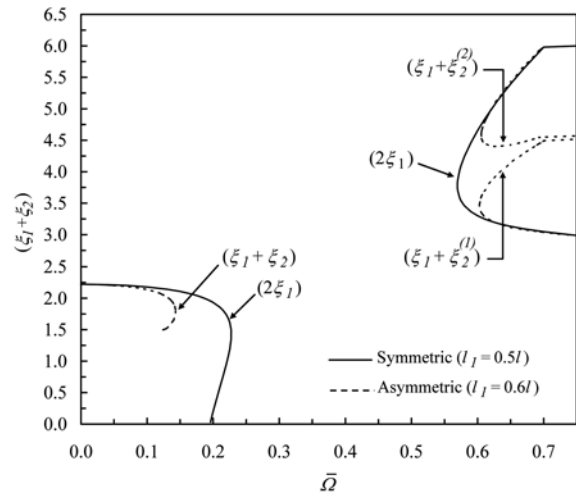


Fig. 8 Variation of total contact length $(\xi_1 + \xi_2)$ with frequency parameter $\bar{\Omega}$ for $l = 6$, for the symmetric and asymmetric loading case

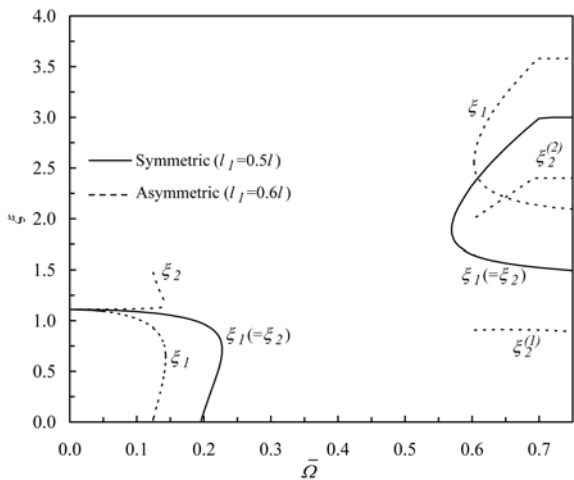


Fig. 9 Variation of the left (ξ_1) and right (ξ_2) side contact lengths with frequency parameter $\bar{\Omega}$ for $l = 6$, for the symmetric and asymmetric case. Note: superscripts (1) and (2) correspond to the first and second solutions, respectively

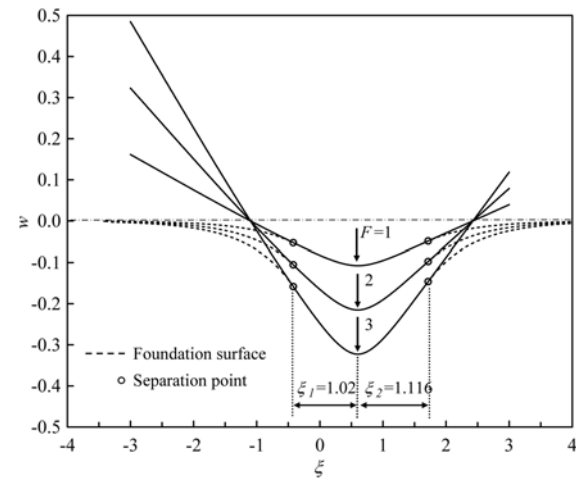


Fig. 10 Deflection curves showing lift-off with $l = 6$, $\bar{\Omega} = 0.1$ and $F = 1; 2; 3$ for the asymmetric case

the range $0.227 < \bar{\Omega} < 0.569$. However, this range becomes larger in the asymmetric case ($0.143 < \bar{\Omega} < 0.603$), as can be seen from Fig. 8 or 9. Fig. 8 shows the variation of the total contact length with respect to the frequency parameter with $l = 6$ for the asymmetric loading. For this beam length, the behavior of the left and right side contact lengths is given in Fig. 9. The symmetric case is also shown for comparison. As before, the left and right contact lengths are summed to obtain the total beam contact length. As seen in Fig. 8, contact length for the asymmetric case is less than that

of the symmetric case at small $\bar{\Omega}$ values. This is because the left (ξ_1) and right (ξ_2) side contact lengths in the asymmetric case are different from each other (see Fig. 9), and the summation of these functions gives smaller values than that of the symmetric case. From Fig. 8, it is also observed that four solutions (four different contact lengths at the same frequency) exist in the asymmetric case for larger values of $\bar{\Omega}$. While two of the solutions exist between the symmetric solutions, the other two solutions are very close to the symmetric ones. As before, these solutions are obtained by summing the left (ξ_1) and right ($\xi_2^{(1)}, \xi_2^{(2)}$) side contact functions given in Fig. 9. Finally, Fig. 10 shows the deflection under different asymmetric loads for a beam length of $l=6$. This figure shows that the beam has clearly lifted off the foundation in both sides. In addition, an increase in the load results in an increase in the displacements without changing the extent of the contact region.

5. Conclusions

The contact lengths and deflections of a finite free-free beam with different lengths and symmetric/asymmetric harmonic loadings on a tensionless Pasternak foundation are discussed. The frequency parameter and the beam length are vital to determining the contact lengths. The loading position is also important, as asymmetric loading results in different left and right contact lengths. The contact length is independent of the magnitude of the load, whereas the deflection profile is directly proportional to it. Depending on the frequency parameter and the beam length, more than one solution (contact length) may exist in the system; i.e., the solution is not unique. The non-uniqueness of the solutions is due to the nonlinearity associated with the existence of the lift-off regions. For a relatively short beam ($l < 5.11$), contact length increases with the frequency parameter and beam length for all solutions. However, contact-length behavior changes considerably if the beam length is increased beyond the critical value. For long beams, there is no solution for some frequency parameter ranges; i.e., the beam does not lift off the foundation. These ranges are larger in the asymmetric case than those of the symmetric case. In addition, it is observed that the contact and non-contact regions interchange at high frequency values for all beam lengths in both loading cases.

References

- Celep, Z., Malaika, A. and Abu-Hussein, M. (1989), "Forced vibrations of a beam on a tensionless foundation", *J. Sound Vib.*, **128**, 235-246.
- Celep, Z. and Demir, F. (2005), "Circular rigid beam on a tensionless two-parameter elastic foundation", *ZAMM-Z. Angew. Math. Me.*, **85**(6), 431-439.
- Celep, Z. and Demir, F. (2007), "Symmetrically loaded beam on a two-parameter tensionless foundation", *Struct. Eng. Mech.*, **27**(5), 555-574.
- Chen, W.Q., Lü, C.F. and Bian, Z.G. (2004), "A mixed method for bending and free vibration of beams resting on a Pasternak elastic foundation", *Appl. Math. Model.*, **28**, 877-890.
- Choros, J. and Adams, G.G. (1979), "A steadily moving load on an elastic beam resting on a tensionless Winkler foundation", *J. Appl. Mech.*, **46**, 175-180.
- Coşkun, İ. and Engin, H. (1999), "Non-linear vibrations of a beam on an elastic foundation", *J. Sound Vib.*, **223**(3), 335-354.
- Coşkun, İ. (2000), "Non-linear vibrations of a beam resting on a tensionless Winkler foundation", *J. Sound Vib.*,

- 236(3), 401-411.
- Coşkun, İ. (2003), "The response of a finite beam on a tensionless Pasternak foundation subjected to a harmonic load", *Eur. J. Mech. A-Solid*, **22**, 151-161.
- Coşkun, İ., Engin, H. and Özmutlu, A. (2008), "Response of a finite beam on a tensionless Pasternak foundation under symmetric and asymmetric loading", *Struct. Eng. Mech.*, **30**(1), 21-36.
- De Rosa, M.A. (1995), "Free vibrations of Timoshenko beams on two-parameter elastic foundation", *Comput. Struct.*, **57**(1), 151-156.
- De Rosa, M.A. and Maurizi, M.J. (1998), "The influence of concentrated masses and Pasternak soil on the free vibrations of Euler beams-exact solution", *J. Sound Vib.*, **212**(4), 573-581.
- Dutta, S.C. and Roy, R. (2002), "A critical review on idealization and modeling for interaction among soil-foundation-structure system", *Comput. Struct.*, **80**, 1579-1594.
- Filipich, C.P. and Rosales, M.B. (2002), "A further study about the behaviour of foundation piles and beams in a Winkler-Pasternak soil", *Int. J. Mech. Sci.*, **44**(1), 21-36.
- Franciosi, C. and Masi, A. (1993) "Free vibrations of foundation beams on two-parameter elastic soil", *Comput. Struct.*, **47**(3), 419-426.
- Hetényi, M. (1946), *Beams on Elastic Foundation*, The University of Michigan Press, Ann Arbor, USA.
- Horibe, T. and Asano, N. (2001), "Large deflection analysis of beams on two-parameter elastic foundation using the boundary integral equation method", *JSME Int. J. A-Solid. M.*, **44**(2), 231-236.
- Ioakimidis, N.I. (1996), "Beams on tensionless elastic foundation: Approximate quantifier elimination with Chebyshev series", *Int. J. Numer. Meth. Eng.*, **39**(4), 663-686.
- Kaschiev, M.S. and Mikhajlov, K. (1995), "A beam resting on a tensionless Winkler foundation", *Comput. Struct.*, **55**(2), 261-264.
- Kerr, A.D. (1964), "Elastic and viscoelastic foundation models", *J. Appl. Mech.-T. ASME* **31**, 491-498.
- Kerr, A.D. and Coffin, D.W. (1991), "Beams on a two-dimensional Pasternak base subjected to loads that cause lift-off", *Int. J. Solids Struct.*, **28**(4), 413-422.
- Lancioni, G. and Lenci, S. (2007), "Forced nonlinear oscillations of a semi-infinite beam resting on a unilateral elastic soil: Analytical and numerical solutions", *J. Comput. Nonlinear Dyn.*, **2**(2), 155-166.
- Lin, L. and Adams, G.G. (1987), "Beam on tensionless elastic foundation", *J. Eng. Mech-ASCE*, **113**, 542-553.
- Maheshwari, P., Chandra, S. and Basudhar, P.K. (2004), "Response of beams on a tensionless extensible geosynthetic-reinforced earth bed subjected to moving loads", *Comput. Geotech.*, **31**, 537-548.
- Malekzadeh, P. and Karami, G. (2008), "A mixed differential quadrature and finite element free vibration and buckling analysis of thick beams on two-parameter elastic foundations", *Appl. Math. Model.*, **32**, 1381-1394.
- Rao, N.V.S.K. (1974), "Onset of separation between a beam and tensionless elastic foundation due to moving loads", *J. Appl. Mech.-T. ASME*, **41**, 303-305.
- Rao, G.V. (2003), "Large-amplitude free vibrations of uniform beams on Pasternak foundation", *J. Sound Vib.*, **263**(4), 954-960.
- Silveira, R.A.M., Pereira, W.L.A. and Gonçalves, P.B. (2008), "Nonlinear analysis of structural elements under unilateral contact constraints by a Ritz type approach", *Int. J. Solids Struct.*, **45**, 2629-2650.
- Tsai, N.C. and Westmann, R.E. (1967), "Beams on tensionless foundation", *J. Eng. Mech-ASCE*, **93**, 1-12.
- Valsangkar, A.J. and Pradhanang, R. (1988), "Vibrations of a beam-column on two-parameter elastic foundation", *Earthq. Eng. Struct., D*, **16**, 217-225.
- Weitsman, Y. (1970), "On foundations that react in compression only", *J. Appl. Mech.-T. ASME*, **37**(7), 1019-1030.
- Weitsman, Y. (1971), "Onset of separation between a beam and tensionless elastic foundation under a moving load", *Int. J. Mech. Sci.*, **13**, 707-711.
- Weitsman, Y. (1972), "A tensionless contact between a beam and an elastic half-space", *Int. J. Eng. Sci.*, **10**, 73-81.
- Zhang, Y. and Murphy, D.K. (2004), "Response of a finite beam in contact with a tensionless foundation under symmetric and asymmetric loading", *Int. J. Solids Struct.*, **41**, 6745-6758.
- Zhaohua, F. and Cook, R.D. (1983), "Beam elements on two-parameter elastic foundations", *J. Eng. Mech-ASCE* **109**, 1390-1402.
- Zhang, Y. (2008), "Tensionless contact of a finite beam resting on Reissner foundation", *Int. J. Mech. Sci.*, **50**, 1035-1041.

Appendix A

When the contact and non-contact regions interchange in the symmetric case, the boundary and continuity conditions become

$$\begin{aligned} \{w_1(\xi)\}_{\xi \rightarrow -\infty} &\rightarrow \text{finite}, \quad w_1(-l_1) = w_2(-l_1), \quad -w_2'''(-l_1) + \frac{4}{\lambda_G} w_2'(-l_1) = \frac{4}{\lambda_G} w_1'(-l_1), \quad w_2''(-l_1) = 0 \\ w_2(-\xi_1) &= w_3(-\xi_1), \quad w_2'(-\xi_1) = w_3'(-\xi_1), \quad w_2''(-\xi_1) = w_3''(-\xi_1), \quad w_2'''(-\xi_1) = w_3'''(-\xi_1) \\ w_3(-\xi_1) &= w_4(-\xi_1), \quad w_3'(-\xi_1) = w_4'(-\xi_1), \quad w_3''(0) = 0, \quad w_3'''(0) = \frac{F}{2}, \quad w_4''(0) = 0 \end{aligned}$$

Due to symmetry, only the left side of the system is considered here. In the above equations, w_1 is the vertical deflection of the shear layer beyond the beam left end, w_2 is the beam deflection in the contact region, and w_3 and w_4 are the vertical deflections of the beam and shear layer in the non-contact region (in the middle part of the beam), respectively. Note that the number of the boundary and continuity conditions becomes 13 for this case.

Appendix B

When the contact and noncontact regions interchange in the asymmetric case, the boundary and continuity conditions on the left and right sides are as follows

On the left side of the system

$$\begin{aligned} \{w_1(\xi)\}_{\xi \rightarrow -\infty} &\rightarrow \text{finite}, \quad w_1(-l_1) = w_2(-l_1), \quad -w_2'''(-l_1) + \frac{4}{\lambda_G} w_2'(-l_1) = \frac{4}{\lambda_G} w_1'(-l_1), \quad w_2''(-l_1) = 0 \\ w_2(-\xi_1) &= w_3(-\xi_1), \quad w_2'(-\xi_1) = w_3'(-\xi_1), \quad w_2''(-\xi_1) = w_3''(-\xi_1), \quad w_2'''(-\xi_1) = w_3'''(-\xi_1) \\ w_3(-\xi_1) &= w_6(-\xi_1), \quad w_3'(-\xi_1) = w_6'(-\xi_1) \end{aligned}$$

On the right side of the system

$$\begin{aligned} \{w_5(\xi)\}_{\xi \rightarrow +\infty} &\rightarrow \text{finite}, \quad w_4(l_2) = w_5(l_2), \quad -w_4'''(l_2) + \frac{4}{\lambda_G} w_4'(l_2) = \frac{4}{\lambda_G} w_5'(l_2), \quad w_4''(l_2) = 0 \\ w_3(\xi_2) &= w_4(\xi_2), \quad w_3'(\xi_2) = w_4'(\xi_2), \quad w_3''(\xi_2) = w_4''(\xi_2), \quad w_3'''(\xi_2) = w_4'''(\xi_2) \\ w_3(\xi_2) &= w_6(\xi_2), \quad w_3'(\xi_2) = w_6'(\xi_2) \end{aligned}$$

Here, w_1 , w_2 , and w_3 are defined as in the symmetric case. However, the deflection of the shear layer in the non-contact region, i.e., in the middle part of the beam, is denoted by w_6 . Also, w_4 and w_5 show the deflections of the beam in the contact region and the deflections of the shear layer beyond the beam right end, respectively. Note that the number of the boundary and continuity conditions becomes 20 for this case.